X-ray imaging of extended magnetic domain walls in $Ni_{80}Fe_{20}$ wires

S. Basu[1], P. W. Fry[2], D. A. Allwood[1*], M. T. Bryan[1], M. R. J. Gibbs[1], T. Schrefl[3], M.-Y. Im[4], P. Fischer[4]

[1] Department of Engineering Materials, University of Sheffield, Sheffield S1 3JD, United Kingdom

[2] Nanoscience and Technology Centre, University of Sheffield, Sheffield S3 7HQ, United Kingdom

[3] St. Poelten University of Applied Sciences, 3100 St. Poelten, Austria

[4] LBNL/CXRO, 1 Cyclotron Road, Berkeley, California 94720, USA

Abstract

We have used magnetic transmission X-ray microscopy to image magnetization configurations in 700 nm wide $Ni_{80}Fe_{20}$ planar wires attached to 'nucleation' pads. Domain walls were observed to inject only across half of the wire width but extend to several micrometers in length. Magnetostatic interactions with adjacent wires caused further unusual domain wall behavior. Micromagnetic modeling suggests the extended walls have Néel-like structure along their length and indicates weaker exchange coupling than is often assumed. These observations explain previous measurements of domain wall injection and demonstrate that magnetic domain walls in larger nanowires cannot always be considered as localized entities.

* Email: d.allwood@sheffield.ac.uk

The study of magnetic domain walls in planar magnetic nanowires has become extremely popular over recent years. Nanowires fabricated from magnetically soft materials such as $Ni_{80}Fe_{20}$ (Permalloy) have magnetization that relaxes along the wire long axis. Furthermore, magnetization can gradually rotate to follow wire corners and allow complex nanowire networks to be designed.[1] Several proposed applications[1-5] are based on the principle of using localized domain walls in magnetically soft nanowires to spatially separate streams of opposite magnetic domains in nanowires. Nanowire logic gates go further in using interactions between domain walls brought together at wire junctions.[1,6]

Domain walls in bulk and thin film ferromagnets vary essentially only in one dimension, taking on either a Bloch or Néel structure, even when undergoing dynamic changes during propagation.[7] Imaging and micromagnetic modeling of the 'head-to-head' domain walls found in soft magnetic nanowires has revealed that they have more complex, two-dimensional structure variation, resulting in a wider diversity of domain wall types. Domain walls in nanowires are loosely classed as being 'transverse' or 'vortex',[8] although the transverse wall structure can vary[9] and multiple vortices are possible within a domain wall.[10] The dynamic structure of domain walls propagating in nanowires can be further complicated by the presence of 'anti-vortex' configurations. These variations are extremely important since they influence how domain walls propagate[8] and interact with geometrical features used to control domain wall position.[11] Domain walls have been observed to stretch up to 1.5 μm under an applied field when pinned on one side of a nanowire,[11] which could pose problems for devices that rely on domain walls remaining close to their typical relaxed widths of 50 – 200 nm.

Here, we discuss high resolution magnetic transmission soft X-ray microscopy (M-TXM) of domain wall processes in patterned Permalloy structures. Specifically, we have studied domain wall injection from large 'nucleation pads' into attached wires and observed domain walls propagating along one side of the wire over distances up to 10 μm before interacting with other wires nearby.

We use micromagnetic modeling to investigate the nature of these highly stretched domain walls, for which the notion of a localized 'head-to-head' structure breaks down. Our results explain previous measurements made on domain wall injection from nucleation pads.[12]

All structures were fabricated from thermally evaporated Permalloy films deposited on 100 nm thick Si_3N_4 membranes using electron beam lithography followed by lift-off in acetone held at 50°C. The structures were 20 nm thick and consisted of 10 μm × 10 μm nucleation pads with wires of width 700 nm attached [Fig. 1]. At a distance of 10 μm from the nucleation pad, the wires passed between two orthogonal wires, each separated from the original wire by 40 nm [Fig. 1], and one of which had a 4 μm × 4 μm nucleation pad attached. This feature was designed as part of a separate study into magnetostatic effects upon domain wall propagation[13] but some particular aspects of the behavior it induces are discussed here. Figure 1 also defines the orthogonal directions *x* and *y*, along which magnetic fields H_x and H_y are applied, respectively.

Magnetic transmission X-ray microscopy (M-TXM) was performed at beamline 6.1.2 at the Center for X-ray Optics, Advanced Light Source in Berkeley, CA.[14] M-TXM uses the differential absorption of polarized X-rays in magnetic materials due to X-ray magnetic circular dichroism (X-MCD) to create magnetization contrast in images. Fresnel zone plates are used as condenser and objective lenses to provide up to 15 nm spatial resolution with an approximately 10 μm diameter field of view, imaged on an X-ray sensitive charge-coupled device (CCD) camera. In this study we used an objective lens providing better than 25 nm spatial resolution. The zone plates were also used to select X-rays with 853 eV photon energy in order to be sensitive to the Ni L_3-edge. Samples are held at an angle of 30° to the X-ray optical axis in order to provide magnetization contrast in the *x*-direction. Electromagnets are used to apply fields H_x and H_y during and between image capture. The signal-to-noise ratio of raw images is improved by averaging several images from the CCD camera, binning adjacent CCD pixels and applying digital smoothing functions. The images shown here are obtained by dividing two raw images obtained under different field conditions to show

changes in magnetization and remove the strong contrast between regions containing magnetic structure and bare substrate. Here, one of the raw images is always under remanent or saturation conditions, so the final image represent the magnetization state of the second raw image. Full details of the experimental arrangement of the microscope can be found elsewhere.[15,16]

Micromagnetic simulations were performed using a hybrid finite element/boundary element code[17] developed by one of us (TS) to solve the Landau-Lifshitz-Gilbert equation of motion.[18] This code has been used previously to solve magnetization dynamics of domain walls in magnetic nanowires[19,20] and is well suited to the calculations required here. We use a graded finite element mesh. The lateral mesh size is 5 nm in the region where domain walls propagate and 20 nm elsewhere. Thus we can model the nanowire system with the accurate magnetostatic fields taking into account the shape of the pads and also resolve domain walls where required. Within one tetrahedral finite element the magnetization is interpolated linearly. Throughout the thickness of the nanowire the element size was 20 nm. Grading the mesh and using elements with a 1:4 aspect ratio results in much faster calculations for these thicknesses than a uniform 5 nm mesh size throughout and tests showed little variation between the two methods for the wires. High aspect ratio finite elements cause no numerical difficulties if proper preconditioning of the arising linear system is done.[17] The material properties of bulk Permalloy were used in the model unless otherwise stated, with exchange stiffness A = 1.3×10^{-11} J.m^{-1}, saturation magnetization M_S = 800 kA.m^{-1}, magneto-crystalline anisotropy K = 0 J.m^{-3} and damping constant α = 0.01. For simulations of switching fields, a linearly increasing magnetic field (1 Oe/ns) was applied parallel to the wire long axis. The dimensions of the simulated structures mimicked the essential features of the experimental structures, although edge roughness was neglected from the model.

Nucleation pads have been used in a wide range of experiments to introduce domain walls into nanowires under magnetic fields much lower than they are generated in free wire ends.[3,12,21-24] This has allowed a number of nanowire devices to be tested without unwanted domain wall

nucleation or device breakdown occurring[6,25,26] and they act as a source of domain walls in magnetic logic and sensor devices.[1,3,24] The initial magnetization reversal of the nucleation pad often leaves a domain wall pinned at the pad-wire junction,[21,22,27,28] and a larger 'injection' field is then required to move the wall into the wire. One study of domain wall injection from nucleation pads[12] found that the nature of domain wall injection depended on the wire width. For narrower (< 320 nm) wires, multi-modal behavior was observed in single-shot hysteresis loops as a stochastic variation of injection fields. For wider (535 nm) wires, stepped magnetization reversal was observed in single-shot hysteresis loops, although the reason for this was unclear.

Our observations of domain wall injection into wires provided some surprising results. Figure 2 shows a sequence of images of a nucleation pad and part of a 700 nm wide wire under increasing axial field, H_x. Upon reaching H_x = 70 Oe, a domain wall enters the wire. However, the injection is anything but uniform; the domain wall stretches for approximately 1.8 μm down the lower half of the wire only, whereas across the top half of the wire the domain wall remains pinned at the wire/pad junction [Fig. 2(a)]. As H_x is increased, the domain wall extends progressively further into the wire [Fig. 2(b) and (c)], reaching a distance of 4.5 μm from the pad when H_x = 120 Oe. Throughout this, the domain wall retains some 90° turns close to the pad and terminates at the upper join between the wire and pad. The domain wall is finally injected across the whole wire when H_x = 130 Oe. The extended domain walls shown in Fig. 2 do not fit the general description of head-to-head walls. Rather, it has a head-to-head structure only where it is orthogonal to the wire length [Fig. 2(e)]. The extended regions lying parallel to the wire instead have a domain configuration either side of the wire more akin to a Bloch or Néel type wall [Fig. 2(e)].

We also moved further along the 700 nm wide wire, away from the nucleation pad, in order to observe how the extended wall interacted with the orthogonal wires. These wires had previously been saturated in the +y-direction. Figure 3(a) shows an extended domain wall approaching the wire cross (H_x = 70 Oe), reaching 10 μm from the pad. Figure 3(b)-(d) are from a separate sequence of

fields but show that at higher applied fields (H_x = 110 Oe), the domain wall reaches the wire cross [Fig. 3(b)]. However, rather than becoming pinned at this point, the stray magnetic field from the ends of the orthogonal wires appears to cause the domain extending into the wire to locally expand across the wire width. The domain continues to expand beyond the cross, reverting back to expansion through half the wire width only. However, now the domain expansion appears on the opposite side of the wire than previously. As the field is increased further, the wire beyond the cross undergoes full magnetization reversal [Fig. 3(c); H_x = 120 Oe] before the wire between the pad and the cross finally switches completely [Fig. 3(d); H_x = 130 Oe]. Similar observations to those in Figs. 2 and 3 were also observed with 400 nm wide wires.

Figure 4(a) and (b) show micromagnetic simulations of a 20 nm thick patterned Permalloy element in which a domain wall is being injected from a 4 μm × 4 μm nucleation pad into a 400 nm wide wire under an applied axial field of 60 Oe. The lower part of the domain wall extends into the nanowire while the upper part remains pinned at the pad/wire junction. This asymmetry is due to the closure domains in the pad above and below the junction with the wire having opposite orientations in the initialized structure before the field was applied. Such end domains are not visible in Fig. 2 but such an interaction is most likely to be the cause of the strong domain wall pinning observed. The domain wall is also observed to have a Néel-type configuration along the wire length. In order to achieve the extended domain wall structure in the calculations we had to reduce the exchange stiffness to $A = 3.0 \times 10^{-12}$ J.m^{-1}. This can be justified by noting that the exchange constant in granular films may be reduced compared to the bulk value[29,30] and using $A = 1.3 \times 10^{-11}$ J.m^{-1} results in domain walls only extending for 650 nm into the wire. Using this value, domain walls are observed to extend by over 2 μm into the wire from the pad, although the precise structure is very different from that observed in Fig. 2. We have estimated the energy of the extended domain walls by performing micromagnetic simulations of a domain wall initialized down the centre of 400 nm wide, 20 nm thick $Ni_{80}Fe_{20}$ rectangular elements of 2 – 4 μm length [Fig. 4(d)], similar to those observed in isolated structures elsewhere.[31] For all wire lengths, the wall relaxed to a Néel-type

configuration and the end domains appeared very similar. The total calculated energy increased linearly with wire length, allowing us to estimate the domain wall energy density as γ = 3.0 mJ.m^{-2} (1.4 mJ.m^{-2} for A = 3.0 × 10^{-12} J.m^{-1}). The domain wall extended to a length of 10 μm in Fig. 3 therefore has an energy = 0.60 fJ (0.28 pJ for A = 3.0 × 10^{-12} J.m^{-1}), and we can assume that the interaction energy between the domain wall and the closure domain in the nucleation pad is of at least this value. However, the creation of the domain wall reduces the total magnetostatic energy (Zeeman + demagnetizing) of the system and can be estimated from the energy terms in the simulations shown in Fig. 4(a) and (b). For the wire dimensions considered here, the magnetostatic energy gain per unit length of the domain wall is estimated to be 0.85 fJ.μm^{-1}, giving an energy reduction of 8.5 fJ for a 10 μm long wall. The modeled domain walls such as in Fig. 4(d) also allow us to estimate a domain wall width of 40 nm by extrapolating the magnetization gradient at the center of the domain wall.

While the extended Néel wall may be unexpected, it does explain our previous observation of stepped hysteresis loops when domain walls were injected from nucleation pads into 500 nm wide wires.[12] This was observed even within single magnetization reversal events, ruling out the simple possibility of stochastic variation in single-step switching field. What now appears to have been happening is injection of a domain across half of the wire width at a low field with subsequent reversal of the other half at a higher field, as observed here. While we do not claim that the extended Néel walls are necessarily typical of domain wall behavior in wires, the trend to wider and thicker wires to promote head-to-head walls with a vortex spin structure[32] for more efficient coupling with spin-polarized currents[33] may result in further similar observations being made. The interaction of the extended wall with the magnetostatic cross (Fig. 3) indicates that the head-to-head/Néel hybrid walls will exhibit unusual behavior in what might otherwise be a well understood magnetic nanowire system, perhaps affecting device performance.

In conclusion, we have used magnetic transmission soft X-ray microscopy (M-TXM) providing 25 nm spatial resolution to image domain wall injection into patterned magnetic wires. Domain wall injection into wider (400 and 700 nm) wires is observed to often take place initially across one half of the wire width only, resulting in a highly extended domain wall with large regions of Néel-type structure. This behavior has wider implications for experiments and devices using patterned magnetic wires with larger cross-sectional dimensions. Future experiments using time-resolved M-TXM may assist in investigating these effects.

Acknowledgements

This work was supported by the EPSRC grants GR/T02959/01 and EP/D056683/1, an EPSRC DTA studentship, and by the Director, Office of Science, Office of Basic Energy Sciences, Materials Sciences and Engineering Division, of the U.S. Department of Energy under Contract No. DE-AC02-05-CH11231.

References

1 D. A. Allwood, G. Xiong, C. C. Faulkner, D. Atkinson, D. Petit, and R. P. Cowburn, Science **309,** 1688 (2005).

2 S. S. P. Parkin, M. Hayashi, and L. Thomas, Science **320,** 190 (2008).

3 M. Diegel, R. Mattheis, and E. Halder, Sensor Letters **5,** 118 (2007).

4 D. Atkinson, D. S. Eastwood, and L. K. Bogart, Appl. Phys. Lett. **92,** 022510 (2008).

5 R. D. McMichael, J. Eicke, M. J. Donahue, and D. G. Porter, J. Appl. Phys. **87,** 7058 (2000).

6 C. C. Faulkner, D. A. Allwood, M. D. Cooke, G. Xiong, D. Atkinson, and R. P. Cowburn, IEEE Trans. Magn. **39,** 2860 (2003).

7 V. L. Sobolev, H. L. Huang, and S. C. Chen, J. Appl. Phys. **75,** 5797 (1994).

8 A. Thiaville and Y. Nakatani, in *Spin Dynamics in Confined Magnetic Structures III*, edited by B. Hillebrands and A. Thiaville (Springer, 2006), p. 161 - 205.

[9] C. W. Sandweg, N. Wiese, D. McGrouther, S. J. Hermsdoerfer, H. Schultheiss, B. Leven, S. McVitie, B. Hillebrands, and J. N. Chapman, J. Appl. Phys. **103,** 093906 (2008).

[10] G. Meier, M. Bolte, R. Eiselt, B. Krüger, D. H. Kim, and P. Fischer, Phys. Rev. Lett. **98,** 187202 (2007).

[11] K. J. O'Shea, S. McVitie, J. N. Chapman, and J. M. R. Weaver, Appl. Phys. Lett. **93,** 202505 (2008).

[12] M. T. Bryan, D. Atkinson, and D. A. Allwood, Appl. Phys. Lett. **88,** 032505 (2006).

[13] S. Basu, P. W. Fry, T. Schrefl, M. R. J. Gibbs, D. A. Allwood, M.-Y. Im, and P. Fischer, in preparation.

[14] http://www.cxro.lbl.gov/BL612/.

[15] P. Fischer, D. H. Kim, W. Chao, J. A. Liddle, E. H. Anderson, and D. T. Attwood, Materials Today **9,** 26 (2006).

[16] P. Fischer, IEEE Trans. Magn. **44,** 1900 (2008).

[17] D. R. Fredkin and T. R. Köhler, IEEE Trans. Magn. **26,** 415 (1990).

[18] D. Suess, V. Tsiantos, T. Schrefl, J. Fidler, W. Scholz, H. Forster, R. Dittrich, and J. Miles, J. Magn. Magn. Mater. **248,** 298 (2002).

[19] M. T. Bryan, T. Schrefl, and D. A. Allwood, Appl. Phys. Lett. **91,** 142502 (2007).

[20] M. T. Bryan, T. Schrefl, D. Atkinson, and D. A. Allwood, J. Appl. Phys. **103,** 073906 (2008).

[21] K. Shigeto, T. Shinjo, and T. Ono, Appl. Phys. Lett. **75,** 2815 (1999).

[22] R. P. Cowburn, D. A. Allwood, G. Xiong, and M. D. Cooke, J. Appl. Phys. **91,** 6949 (2002).

[23] A. Yamaguchi, S. Nasu, H. Tanigawa, T. Ono, K. Miyake, K. Mibu, and T. Shinjo, Appl. Phys. Lett. **86,** 012511 (2005).

[24] D. A. Allwood, G. Xiong, and R. P. Cowburn, J. Appl. Phys. **100,** 123908 (2006).

[25] C. C. Faulkner, M. D. Cooke, D. A. Allwood, D. Petit, D. Atkinson, and R. P. Cowburn, J. Appl. Phys. **95,** 6717 (2004).

[26] D. A. Allwood, G. Xiong, and R. P. Cowburn, J. Appl. Phys. **101,** 024308 (2007).

[27] M. Brands and G. Dumpich, J. Phys. D **38,** 822 (2005).

[28] L. Thomas, C. T. Rettner, M. Hayashi, M. Samant, S. S. P. Parkin, A. Doran, and A. Scholl, Appl. Phys. Lett. **87,** 262501 (2005).

[29] D. Süß, T. Schrefl, J. Fidler, and J. N. Chapman, J. Magn. Magn. Mater. **196-197,** 617 (1999).

[30] R. H. Victora, Phys. Rev. Lett. **58,** 1788 (1987).

[31] X. Liu, J. N. Chapman, S. McVitie, and C. D. W. Wilkinson, J. Appl. Phys. **96,** 5173 (2004).

[32] Y. Nakatani, A. Thiaville, and J. Miltat, J. Magn. Magn. Mater. **290-291,** 750 (2005).

[33] M. Kläui, P.-O. Jubert, R. Allenspach, A. Bischof, J. A. C. Bland, G. Faini, U. Rüdiger, C. A. F. Vaz, L. Vila, and C. Vouille, Phys. Rev. Lett. **95,** 026601 (2005).

Figure Captions

Figure 1 Schematic diagram of Permalloy structure comprising a nucleation pad and attached 700 nm wide wire. The free wires are separated from the main wire by 40 nm.

Figure 2 M-TXM images of domain wall injection into a 700 nm wide wire under H_x = (a) 70 Oe, (b) 100 Oe, (c) 120 Oe, and (d) 130 Oe. (e) Schematic diagram of magnetization configuration (arrows) of a partially-injected domain wall in a magnetic nanowire attached to a nucleation pad.

Figure 3 M-TXM images of domain wall propagation through a magnetostatic wire cross under H_x = (a) 70 Oe, (b) 110 Oe, (c) 120 Oe, and (d) 130 Oe. Note that (a) was obtained from a separate sequence from the other images.

Figure 4 Micromagnetic models of domain walls in 20 nm thick Permalloy wires. The arrows represent the local magnetization direction while the color represents the magnetization component along the wire axis. (a) Simulation of a domain wall entering a 400 nm wide wire from a 4 μm × 4 μm injection pad under an applied field H = 60 Oe. (b) Magnified view of the wire/pad junction in (a). Magnified view of a similar simulation to (a) but with exchange stiffness A = 3×10^{-12} J.m^{-1} and H_x = 63 Oe. (d) Simulation of a relaxed domain wall along the length of a 3 μm long, 400 nm wide wire (A = 1.3×10^{-11} J.m^{-1}).

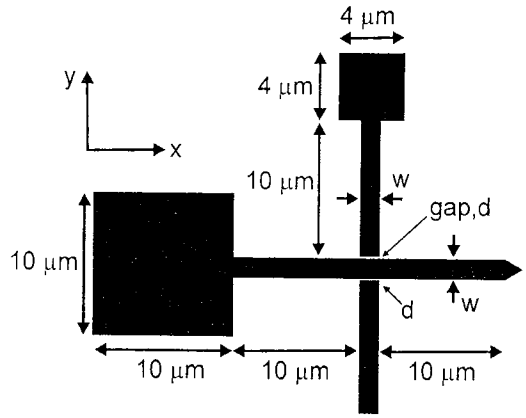

Figure 1

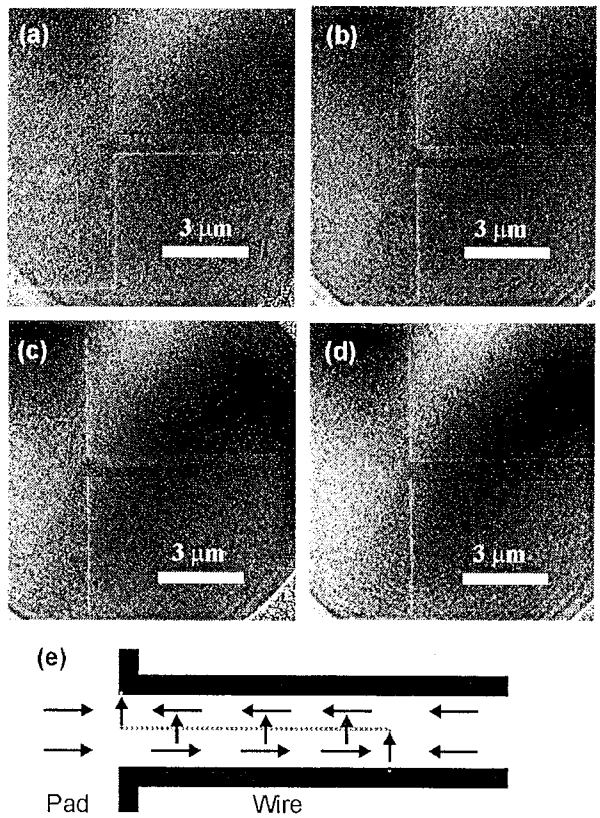

Figure 2

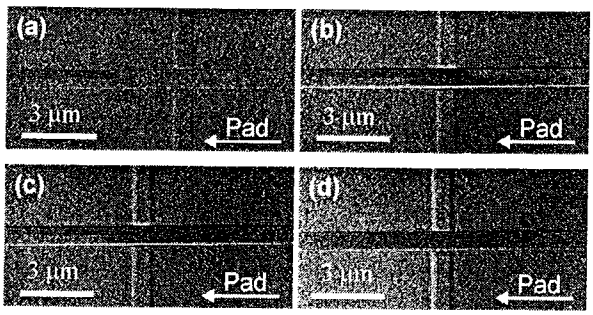

Figure 3

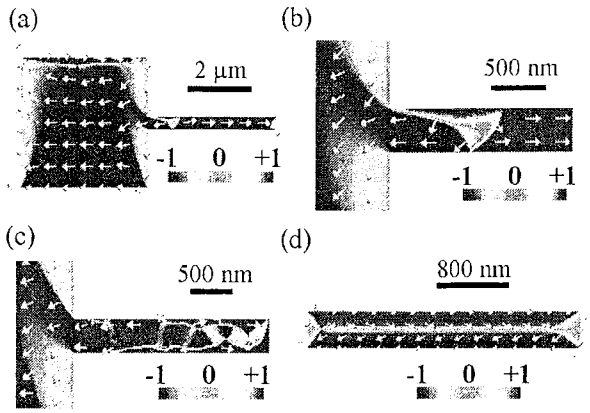

Figure 4